Lattice model for the calculation of the angle of repose from microscopic grain properties

J. J. Alonso,[1,2] J.-P. Hovi,[3] and H. J. Herrmann[1,3]
[1]*Laboratoire P.M.M.H., École Supérieure de Physique et Chimie Industrielles, 10 rue Vauquelin, 75005 Paris, France*
[2]*Departamento de Física Aplicada I, Universidad de Málaga, E-29071 Málaga, Spain*
[3]*ICA 1, University of Stuttgart, Pfaffenwaldring 27, 70659 Stuttgart, Germany*
(Received 22 October 1997)

We study a simple lattice model for granular heap, which aims at calculating the macroscopic angle of repose from the microscopic grain properties. The model includes the effects of dissipation of the energy in the particle-particle collisions, and sticking of the particles to the pile. We obtain that, due to the discretization of the space, the angle of repose of the pile behaves as a complete *devil's staircase* as a function of the model parameters. We present numerical and analytical considerations which characterize the properties of this staircase. [S1063-651X(98)09606-8]

PACS number(s): 81.05.Rm

I. INTRODUCTION

The heap of dry granular material is of interest for practical applications, but also as a paradigm in fundamental research. Typical questions include (size or shape) segregation [1–3], avalanches [4,5], and the shape of the heap in two and three dimensions [6–8]. Indeed, sandpiles are almost perfect cones with a well-defined angle of repose, which depends on gravity and on the characteristics of the material, including density [9], humidity [10], packing history, and boundary conditions [8]. However, to our knowledge, no systematic experimental study of the dependence of the angle of repose on the material properties, like the restitution coefficient, the shape, or the surface roughness of the grains, has been performed. It is also a striking fact that the calculation of the macroscopic angle of repose from the microscopic properties of the grains has eluded solution. Additionally, watching carefully, one notices that at the very bottom of a two-dimensional heap the surface profile has a logarithmic correction to this simple conelike behavior [6].

Understanding these phenomena poses a major challenge for research in granular media. In this respect simple models have an important role by allowing one to investigate the system in great detail. They also often serve as a basis towards more realistic simulations of the granular systems. In fact, the use of such simple systems has already revealed many successful characterizations of the crucial interactions underlying different phenomena; for example, Refs. [1–3,6].

In this paper we study a simple lattice model for a pile of dry granular media (say sand, for example). The phenomenological model includes the considerations of the dissipation of energy in the particle-particle collisions, and the sticking of the particles to the pile. At the steady state this deterministic model evolves to a pile, where the angle of repose depends on the dissipation and the shape of the granulates. Thus the present model may help to understand how such properties affect the angle of repose in heaps of granulates. To our knowledge, this constitutes the first model which attempts to calculate the macroscopic angle of repose directly from the microscopic grain properties.

In our model, we find that, due to the discretization, the angle of repose of the pile behaves as a complete *devil's staircase*, which has the peculiar property that the function varies only on a set of zero linear measure. Such staircases have been encountered repeatedly in many contexts of very different physical nature: for example, current-voltage characteristics of Josephson junctions [11,12], superfluid density in ^{4}He thin films [13], and polytypic periodic structures in several metallic compounds, such as Ag_3Mg, CuAu, and Cu_3Pt [14]. For a discussion about devil's staircases in these, and other, physical systems see Ref. [15]. There are also at least two theoretical models where such devil's staircases emerge. The first is a one-dimensional (1D) Ising system with long-range repulsive interactions [16], for which the ratio of the up and down spins varies as a complete devil's staircase as a function of the external field. The second is the axial next-nearest-neighbor Ising (ANNNI) model [17], which may qualitatively explain the polytypic structures in the above mentioned metallic compounds [18].

In this work we present numerical and analytical considerations which characterize the properties of the present staircase. We find that the sizes of the steps on the surface depend on the properties of the granulates in a complicated manner, and this results in a fascinating hierarchical structure in the angle of repose. We also discuss some analogies which arise between the present model and the Ising model mentioned above.

The rest of this paper is organized as follows. We introduce the model in Sec. II, where the basic concepts are discussed in more detail. This section is followed by the presentation of our numerical and analytical results in Sec. III. The connection between the current model and the one-dimensional Ising model are discussed in Sec. IV. Finally, the paper is concluded in Sec. V.

II. MODEL

For simplicity, we consider a one-dimensional pile where the particles are located at $x=0,1,2,\ldots$, measured in the units of the particle diameter (see Fig. 1). We monitor the height of the pile $h(x)$, which also denotes the current number of the particles at the position x, and, in particular, the macroscopic angle of the repose γ, which is the average slope of the pile.

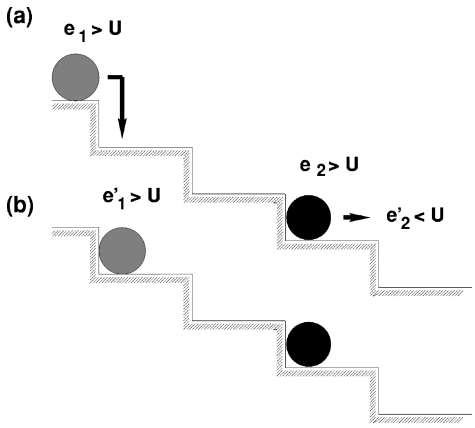

FIG. 1. Schematic view of the evolution of the pile. (a) Gray particle enters the system with the energy e_1, and black particle is falling down the pile with energy e_2. As shown by arrows, the particles try to propagate to the next location in the pile. (b) The particles gain energy in the gravitational field, but a fraction of the energy is dissipated in the particle-particle collisions. Final energy, $e_i'=(e_i+\Delta h_i)r$ $(i=1,2)$, is compared to the threshold value U. Here $e_1'>U$ and gray particle moves on to $x=1$, but $e_2'<U$, hence the black particle remains in its previous position. (For illustration only, in practical simulations we follow only one particle at a time.)

There is a constant flow of particles to the left hand edge, i.e., to $x=0$, for which it is convenient to scale time such that the rate of the particle flow equals one particle per unit time. These particles enter the system with a fixed initial energy e_0. The initial energy is assumed to be independent of $h(0)$, and sufficiently large as compared to other energy scales in the model (see below), which corresponds to an experimental situation where the particles are dropped well above the pile.

The evolution of the pile is determined by energetic considerations. Consider a particle which sits at position x with energy e_i (for illustration, see Fig. 1). In order to propagate to location $x+1$, the particle has to overcome a potential barrier U, which simulates the friction between the moving particle and the pile. Thus U mainly considers the roughness and the shape of the particles. Should the particle succeed in moving to $x+1$, it would (typically) gain energy in the gravitational field by $\Delta h\equiv h(x)-h(x+1)$, but a fraction of the total energy becomes dissipated in the collision with the particles in the pile at $x+1$. This energy dissipation in the particle-particle collisions is determined by the coefficient of the restitution $r\leqslant 1$, which is a material dependent constant. Thus the energy of the particle after moving to $x+1$ would be given by

$$e_i'=(e_i+\Delta h)r. \tag{1}$$

This energy is compared with the potential barrier U. If $e_i'\geqslant U$, the particle propagates to $x+1$ conserving its energy, and similar considerations are repeated in order to decide if it may propagate forwards. However, if $e_i'<U$, the particle sticks in the current location, $h(x)$ is increased by unity, and a new particle is released to the system at $x=0$.

For given (r,U), this deterministic model evolves into a steady state, from which physical observables, such as the global angle of repose $\gamma(r,U)$, can be determined. Within this simple model, the dependence of $\gamma(r,U)$ gives information on how the angle of repose depends on the properties of the granular system, namely, the shape (U) and dissipation (r) between the granulates.

III. RESULTS

The most accessible physical observable is the angle of repose, which characterizes the shape of the pile, as a function of the physical parameters $\gamma=\gamma(r,U)$. To determine $\gamma(r,U)$, we have performed numerical simulations as well as analytical calculations.

A. Numerical results

We performed extensive numerical simulations collecting data for several values of (r,U) by fixing r and varying U. Our first observation is that, indeed, the model evolves towards a steady state which has a well-defined macroscopic angle of repose, whose value depends on the physical characteristics of the grains. In addition, our simulations show that γ does not depend on the initial energy $e_0\geqslant U$, as long as it is fixed. The effects which arise if e_0 is chosen from a (say, bimodal) distribution are discussed elsewhere [19].

The results for $\gamma(r,U)$, as a function of $U(1-r)/r$, are shown in Fig. 2. A striking feature of this figure is that γ shows a constant value for a wide range of U for a fixed r. In fact, these numerical results indicate that $\gamma(r,U)$ is described by a devil's staircase, which varies only on a set of zero linear measure. This is due to the fact that since the height of the pile and the position x are restricted to integer values, γ may achieve only rational values. However, since there is no other *a priori* restriction for γ, we assume below that γ may have all rational values.

For illustration, Fig. 3 shows a typical steady state profile of the sandpile. It can be seen that γ depends on the steps on the surface, i.e., regions where $\Delta h>0$. Specifically, we find numerically that the steady state of the model is a periodic structure for which the surface profile descends by repeating one ''unit cell'' of steps along the pile. The angle of repose is determined by the number (N) and the sizes of these steps in the unit cell of length L.

B. Analytical results

In this subsection we present our analytical calculation of the $\gamma(r,U)$. We start by deriving the connection between the sizes of the steps of the surface and the magnitude of γ (see Sec. III B 1). This leads us to conclude that for noninteger values of γ, $\mathrm{int}(\gamma)=\mathrm{int}[U(1-r)/r]$, where $\mathrm{int}(x)$ gives the integer part of x. Therefore, for simplicity, we continue with a detailed analysis of the case $0<\gamma<1$ (see Sec. III B 2). These calculations are performed in the ''energy space,'' where we consider the energy of a test particle which falls down the pile. Guided by our numerical simulations, we postulate that these energies form a periodic sequence $\{e_i\}$, which has the same periodicity as the surface profile. Using this assumption we are able to form a closed set of equations, from which the behavior of $\gamma(r,U)$ can be determined. We verify numerically that this theoretical reasoning is in agreement with the simulation results. Additionally, the consider-

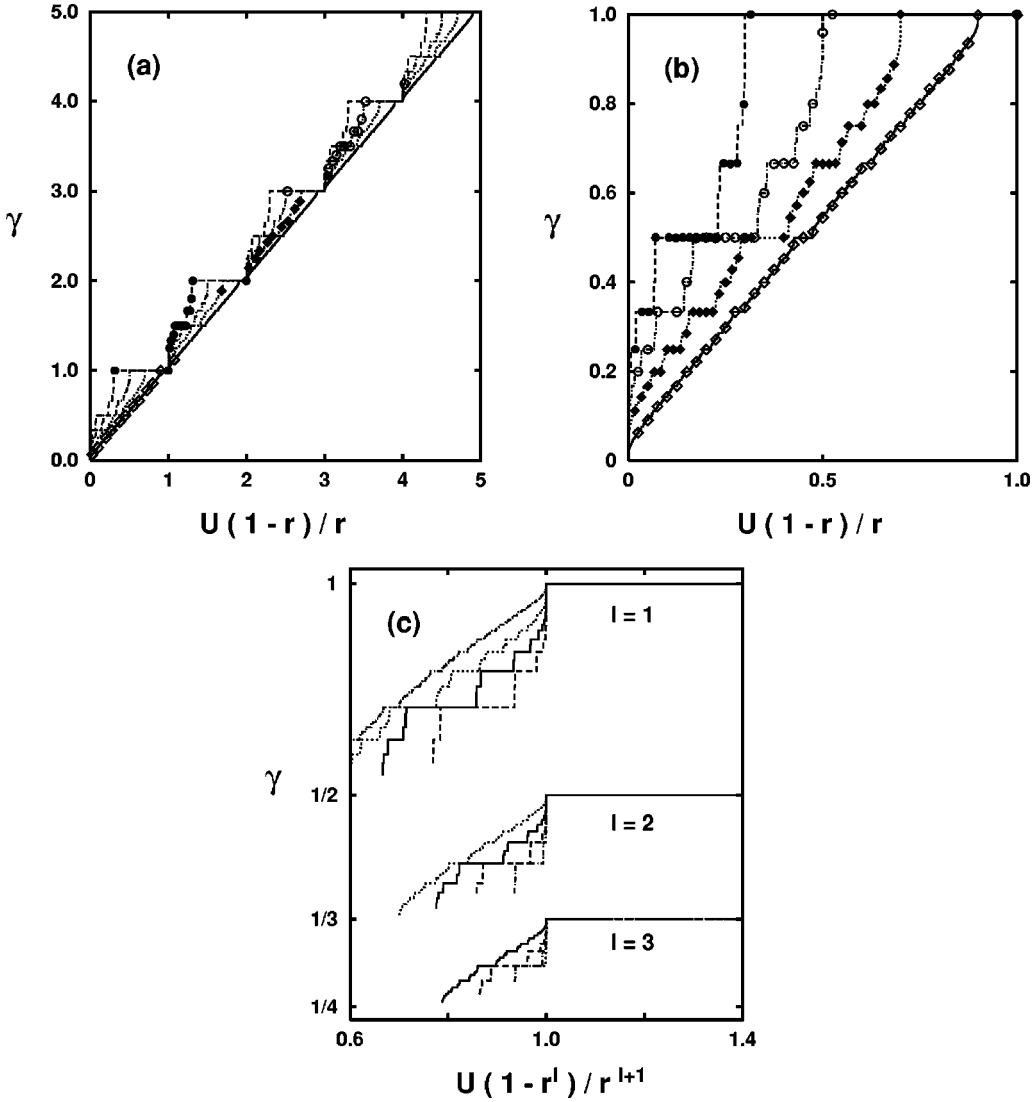

FIG. 2. (a) Numerically measured angle of repose $\gamma(r,U)$ as a function of $U(1-r)/r$ for $r=0.3$ (●, dashed line), 0.5 (○, dashed-dotted line), 0.7 (♦, dotted line), and $r=0.9$ (◇, solid line). The lines display the $\gamma(r,U)$ as calculated from the numerical iteration of Eqs. (23) and (24) (see the text for details). In particular, the data agree well with Eq. (3), which gives $n-1<\gamma<n$ as $n-1<U(1-r)/r<n$. (b) The same data as in (a), but enlarged to show the range $0<\gamma\leqslant 1$ in more detail. The lines are from numerical iteration of Eqs. (4) and (7). (c) The same data as in (b), but γ plotted vs $\bar{U}=U(1-r^l)/r^{l+1}$ in order to show the structure of the staircase in the range $r^{l+1}/(1-r^{l+1}) \leqslant U \leqslant r^l/(1-r^l)$, where $l=\mathrm{int}\{\ln[U/(U+1)]/\ln r\}$, more clearly. From the top to bottom, the data have $l=1,2,3$. If $1<\bar{U}<1/r$, $\gamma=1/l$, but for $(1-r^l)/(1-r^{l+1})<\bar{U}<1$ we find a nontrivial γ in the range $1/(l+1)<\gamma<1/l$.

ations of Sec. III B 2 can be straightforwardly generalized for all $\gamma>0$. These extensions to general γ are summarized in Sec. III B 3.

1. The connection between the step sizes and γ

Consider a particle which is falling down the surface and encounters a step of height $n-1\geqslant 0$. The condition that the particle remains at the current position i and creates a step of height n is given by $e_i'=(e_i+\Delta h)r=(e_i+n-1)r<U$. However, we know that $e_i\geqslant U$ because the particle has been able to propagate to location i. Using this information, we find the estimate, $[U+(n-1)]r<U$, which yields that

$$U>\frac{(n-1)r}{1-r} \tag{2}$$

before steps of size n can be generated. Equation (2) also states that the larger U the larger steps there are on the surface. In particular, at $U=[(n-1)r]/(1-r)$ we have only steps of size $n-1$, since no steps of size n can be created yet, but all the smaller steps are growing since there is a possibility that a particle may not gain enough potential energy to overcome the energy barrier. By induction we deduce that for

$$\frac{(n-1)r}{1-r}<U<\frac{nr}{1-r}, \tag{3}$$

the steady state surface has a mixture of steps of sizes $n-1$ and n. The proper physical picture of the inequality Eq. (3) indicates that for $U=(n-1)r/(1-r)$ all sites have a step of size $n-1$, i.e., $\gamma=n-1$. However, for larger U, also

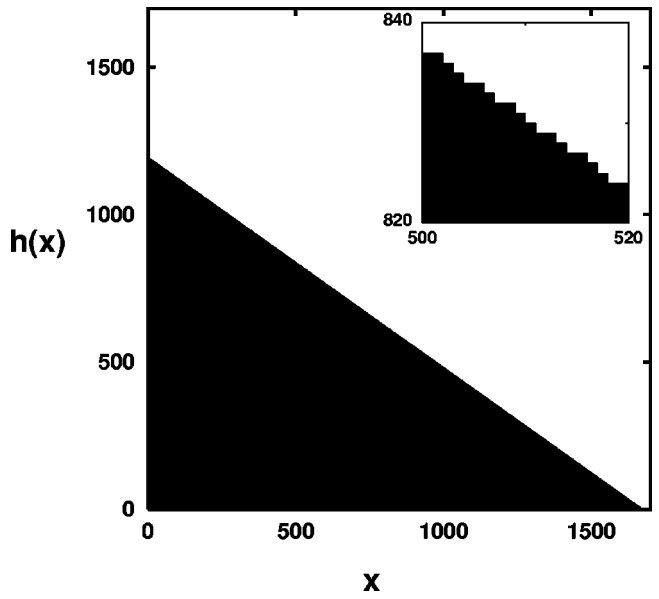

FIG. 3. A simulated surface profile after 10^6 particles. In this example $(r,U)=(1/2,0.43)$ which yields $\gamma=5/7$. The inset shows an enlarged portion of the surface for $500<x<520$, which reveals the periodic small scale structure of the surface in more detail.

steps of size n appear, and their density increases as U grows towards the upper limit of inequality Eq. (3), i.e., $\gamma\to n$ as $U\to nr/(1-r)$. These results agree well with our numerical data shown in Fig. 2(a).

Equation (3) indicates that the sizes of the steps on the surface are determined by U. Since all the sites have a step of size $n-1$ or n, this also demonstrates that in large length scales the steady state surface is very smooth (see Fig. 3), and the average angle of repose γ is a well-defined quantity.

2. Analysis of the case $0<\gamma<1$

(a) Formulation of the problem in terms of the functional iteration. We now turn to a more detailed analysis for $0<\gamma<1$ [see Fig. 2(b)]. As mentioned above, we find numerically that the typical feature of the model is that the steady state of the pile forms a periodic construction, where there are $N\geqslant 1$ steps, of size one (since $0<\gamma<1$), distributed along a basic unit of length L. Obviously we have $\gamma=N/L$, where N and L do not share common factors because L is chosen to be the size of the shortest repeatable unit. Now, it is important to notice that such a periodic steady state surface can be quantitatively characterized by considering the energies of a test particle which is falling down the surface. This test particle is allowed to propagate through the unit cell, and we consider specifically the energy e_i on the top of the ith step in the unit cell (see Fig. 4). Guided by our numerical simulations, we expect that the sequence of energies $\{e_i\}$ has the same periodicity of N steps as the surface profile. Thus we need to solve the recursion relation for e_i,

$$U\leqslant e_{i+1}=(e_i+1)r^{l_i}<U/r, \tag{4}$$

where l_i is the distance between the $(i,i+1)$th steps, $L=\Sigma_{i=1}^{N}l_i$, using periodic ''boundary condition''

$$e_{N+1}=e_1, \tag{5}$$

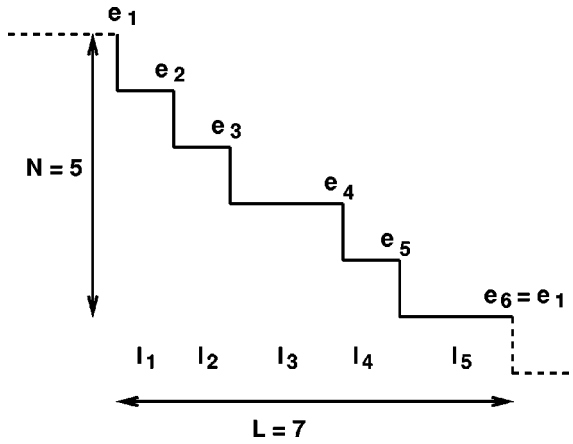

FIG. 4. Notation used in the analytic calculations. This example corresponds to the simulated surface shown in Fig. 3. The unit cell of length $L=7$ has $N=5$ steps, which are labeled using index $i=1,\ldots,N$. These steps have distances l_i, which obey $L=\Sigma l_i$; here $l_1=l_2=l_4=1$, and $l_3=l_5=2$. The energy of a test particle on the top of the ith step is denoted by e_i. We aim at finding a periodic solution for the energies using the boundary condition Eq. (5).

which describes the periodicity of the surface in the ''energy space.'' We emphasize that our assumption, Eq. (5), is a strong relation which determines the number of algebraically independent variables in the sequences $\{e_i\}$, $\{l_i\}$.

We can solve inequality (4) for l_i, and find that the distances between the steps are determined by e_i,

$$\frac{\ln[U/(e_i+1)]}{\ln r}-1<l_i\leqslant\frac{\ln[U/(e_i+1)]}{\ln r}. \tag{6}$$

Because l_i's may have only integer values, Eq. (6) yields

$$l_i=\mathrm{int}\left(\frac{\ln[U/(e_i+1)]}{\ln r}\right). \tag{7}$$

For any (r,U), the angle of repose

$$\gamma(r,U)=\frac{N}{\sum_{i=1}^{N}l_i} \tag{8}$$

is given by solving Eqs. (4), (5), and (7) for unknowns $\{N,l_i,e_i\}$.

(b) Explicit solution of Eqs. (4), (5), and (7). Unfortunately, due to the fact that l_i may have only integer values, the explicit solution of Eqs. (4), (5), and (7) for $\gamma(r,U)=\tilde{\gamma}(\{N,l_i,e_i\})$ is possible only in the simplest cases. In particular, if $N=1$,

$$U\leqslant e_2=(e_1+1)r^{l_1}=e_1<U/r. \tag{9}$$

We can solve Eq. (9) similarly to Eq. (6), and using the fact that $U\leqslant e_1\leqslant U/r$, we find

$$\frac{\ln[U/(U+r)]}{\ln r}<l_1\leqslant\frac{\ln[U/(U+1)]}{\ln r}, \tag{10}$$

$$e_1=\frac{r^{l_1}}{1-r^{l_1}}. \tag{11}$$

Since l_1 may have only integer values, Eq. (10) implies that

$$l_1=\gamma^{-1}=l\equiv\mathrm{int}\left(\frac{\ln[U/(U+1)]}{\ln r}\right), \tag{12}$$

given that the periodic boundary conditions, $U\leqslant e_2=e_1=r^l/(1-r^l)<U/r$, are satisfied, i.e., the barrier has to obey

$$U_{\min}(1/l)=r\frac{r^l}{1-r^l}<U\leqslant\frac{r^l}{1-r^l}=U_{\max}(1/l). \tag{13}$$

By inspection one realizes that Eq. (13) is equivalent to the condition that there exists an integer l, which satisfies Eq. (10). If such an integer l exists, Eq. (12) represents the exact solution for Eqs. (4) and (7), $\gamma^{-1}=l$. Indeed, our data shown in Fig. 2(c) are fully compatible with this expectation. This also shows that at least for the particular case $\{N,l_i,e_i\}=\{1,l,r^l/(1-r^l)\}$, the solution of Eqs. (4), (5), and (7), i.e., $\gamma=1/l$, depends on U only via the dimensionless parameter l.

For other values of (r,U) one needs to find a solution with higher periodicity. Since the sequence $\{e_i\}$ is periodic with a period N, the recursion relation Eq. (9) can be generalized to

$$e_i=\frac{1}{1-r^L}\sum_{j=1}^{j=N} r^{x_{i,i+j}}, \tag{14}$$

where $x_{i,i+j}$ is the distance between the ith and $(i+j)$th step, particularly $x_{i,i+N}=L$, and all N energies in the sequence $\{e_i\}$ are different. This oscillatory behavior of $\{e_i\}$ is due to the lack of the matching distance l according to Eq. (10). In this case the steps of the surface appear with two different intervals l and $l+1$, where each l_i may have either one of these values, depending on that which fulfills the condition $U\leqslant e_{i+1}=(e_i+1)r^{l_i}\leqslant U/r$. Such an interplay between the l_i's leads to a nontrivial angle of repose $(l+1)^{-1}<\gamma<l^{-1}$ if $r^{l+1}/(1-r^{l+1})<U<r[r^l/(1-r^l)]$ [see Fig. 2(c)].

(c) The regions of stability for Eqs. (4), (5), and (7). The trivial solution given in Eqs. (12) and (13) gives a solid reason to expect that generally, for fixed r, there is a range of potential barriers $]U_{\min},U_{\max}]$, which has the same solution $\{N,l_i,e_i\}$, and therefore yields the same angle of repose. However, the explicit solution for $U_{\min,\max}$ is possible only by considering the general form of the sequence $\{e_i\}$. In the Appendix we give a formula for $U_{\min,\max}(\gamma,r,l)$ if $\gamma=(1+p)/[(1+p)l+1]$, where either p or p^{-1} is an integer, but the general solution (for which p is an arbitrary rational number) of $U_{\min,\max}$ becomes very tedious, and not at all that informative. These complications are mainly due to the fact that we do not know how N could be simply determined from the grain properties (r,U).

In this case, however, a lot of information is revealed by considerations of the minimum and maximum values of e_i's alone. For this purpose the analysis of the sequence $\{e_i\}$ is easiest to illustrate using a geometrical construction. For example, Fig. 5 shows the result of the computer simulation at

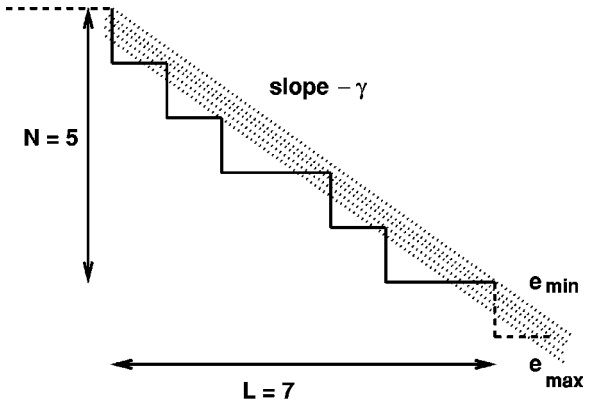

FIG. 5. An illustration of an energy profile for the test particle. In this example $(r,U)=(1/2,0.43)$ which yields $\gamma=5/7$. The dotted lines, which correspond to the five different energy levels in $\{e_i\}$, have slope $-\gamma$. In particular, $\min\{e_i\}$ ($\min\{e_i\}$) is represented by the line on the top (bottom). This geometrical construction verifies that $x_{i,i+j}=d=\mathrm{int}\{j/\gamma\}$ or $d+1$.

$(r,U)=(1/2,0.43)$, which parameters give the depicted surface profile with $\gamma=5/7$. We take every step and draw a line through the hip of that step with slope $-\gamma$. In this example, this kind of the procedure gives that there are five distinct parallel lines which are tangential to the surface. This represents the fact that five consecutive steps, or five different energies e_i, define the smallest repeatable unit of the surface. It is easy to see that in the general case there are N such lines, which represent the N different energies in the sequence $\{e_i\}$. In particular, since the energy increases (decreases) if $l_i=l$ ($l_i=l+1$), one realizes that the minimum (maximum) energies of $\{e_i\}$ are represented by the highest (lowest) lying lines. By inspection we find that this geometrical construction shows that generally $x_{i,i+j}$, for $j<N$, may have two values, either $x_{i,i+j}=d=\mathrm{int}\{j/\gamma\}$ or $d+1$, depending on whether the corresponding line cuts the tip of the $(i+j)$th step below or above. However, one should note that since the lines cut the tip of a step exactly after every N steps we have always $x_{i,i+N}=L$. Let us now consider specifically the minimum and maximum energies which have

$$x_{i,i+j}=\mathrm{int}\left(\frac{j}{\gamma}\right)+1 \quad \text{for all } j<N, \text{ if } e_i=\min\{e_i\}, \tag{15}$$

$$x_{i,i+j}=\mathrm{int}\left(\frac{j}{\gamma}\right) \quad \text{for all } j<N, \text{ if } e_i=\max\{e_i\}. \tag{16}$$

Thus, using Eq. (14), we find

$$\min\{e_i\}=\frac{1}{1-r^L}\left(\sum_{j=1}^{j=N-1} r^{\mathrm{int}\{j/\gamma\}+1}+r^L\right), \tag{17}$$

$$\max\{e_i\}=\frac{1}{1-r^L}\left(\sum_{j=1}^{j=N-1} r^{\mathrm{int}\{j/\gamma\}}+r^L\right). \tag{18}$$

Assuming that all barriers in the range $]U_{\min}(\gamma),U_{\max}(\gamma)]$ yield the same $\{N,l_i,e_i\}$, i.e., the same γ, Eqs. (17) and (18) determine the length of this interval.

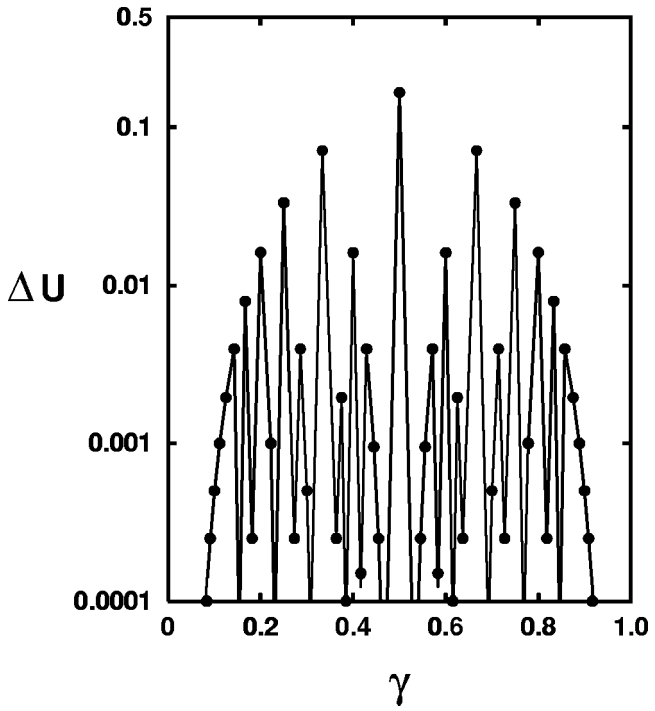

FIG. 6. Numerically measured $\Delta = U_{\max} - U_{\min}$ vs $\gamma = N/L$ for $r = 0.5$ (●) (for clarity, only those values of γ for which $\Delta U > 10^{-4}$ are shown). The solid lines display Eq. (20). Our results for other values of (r,U) show similar behavior.

Since all energies $\{e_i\}$, particularly $\min\{e_i\}$ and $\max\{e_i\}$, are bounded within $[U, U/r[$, for given U, we have $U \leqslant \min\{e_i\} \leqslant \max\{e_i\} < U/r$. On the other hand, we expect that there is a one-to-one correspondence between γ and the N different energies in the sequence $\{e_i\}$. Thus, for given sequence $\{e_i\}$ (i.e., for given γ), the potential barrier must obey

$$r \max\{e_i\} \leqslant U \leqslant \min\{e_i\}. \tag{19}$$

Using Eqs. (17) and (18) we find that the length of the range of U's which is compatible with Eq. (19) is given by

$$\Delta U(\gamma) \equiv U_{\max}(\gamma) - U_{\min}(\gamma) = \frac{r^L(1-r)}{1-r^L}, \tag{20}$$

which imposes that the range of U's which correspond to the same $\gamma = N/L$ is completely determined by the length of the period in real space. As shown in Fig. 6, Eq. (20) agrees excellently with our numerical data.

(d) Completeness of the devil's staircase. Having derived Eq. (20) assuming the unique mapping between interval $]U_{\min}(\gamma), U_{\max}(\gamma)]$ and $\{e_i\}$, we can now check the completeness of the present staircase. Suppose that γ gets *all* the rational values $0 < \gamma \leqslant 1$ for $0 < U \leqslant r/(1-r)$, and add all the intervals $\Delta U(\gamma)$ together:

$$S = \sum_{\gamma \in Q} \Delta U(\gamma) = \sum_{L=1}^{\infty} \phi(L) \frac{r^L(1-r)}{1-r^L}, \tag{21}$$

where $\phi(L)$ is Euler's totient function, which counts the number of primes modulo L (i.e., the number of rational numbers of the form N/L, where N and L do not share any common factors). Using the relation $\Sigma_{L=1}^{\infty} \phi(L) r^L/(1-r^L) = r/(1-r)^2$, $|r| < 1$, which is a generating function for ϕ [20], we find that

$$S = \frac{r}{1-r}, \tag{22}$$

which agrees with Eq. (3) for the allowed range of U's for which $0 < \gamma \leqslant 1$. Thus we find that the commensurate values of γ completely fill the available phase space in U, i.e., the present staircase is complete.

(e) Numerical verification of Eqs. (4), (5), and (7). Iteration of Eqs. (4), (5), and (7) is very easy to implement numerically. In the numerical work, however, it is easiest to replace the periodic ''boundary conditions'' for the energy by the initial condition $e_1 = U$, and compute the angle of repose as the limit $\gamma = \lim_{k \to \infty} k/\Sigma_{i=1}^{k} l_i$. This method overcomes the difficulty of solving Eq. (5), but does not affect the results for γ since for large k the angle becomes calculated over many cycles. For illustration, the solid lines in Fig. 2(b) show the results for γ using the numerical iteration of Eqs. (4) and (7). Indeed, from this comparison we see that the iterates of γ agree excellently with the results from the straightforward simulations. Additionally, the iterates already converge for $k = 10^3$, which speeds up the computations by a factor of 10^3, since otherwise one needs to consider piles of 10^6 particles in order to generate a reasonably large system for the determination of γ.

In order to get a more detailed insight into the structure of Eqs. (4) and (7), we repeated these numerical iterations monitoring also the energies e_i and distances between the consecutive kinks l_i. These simulations confirm numerically the previous assumption that the recursion relations Eqs. (4) and (7) yield periodic solutions $\{e_i\}$ and $\{l_i\}$, for which there is a one-to-one correspondence between γ and the variables $\{N, l_i, e_i\}$, i.e., there is a mapping $\gamma(r,U) = \tilde{\gamma}(\{N, l_i, e_i\})$. Specifically, the plateaus in Fig. 2, which yield the same γ for $U_{\min}(\gamma) \leqslant U \leqslant U_{\max}(\gamma)$, are due to the fact that the solution for $\{N, l_i, e_i\}$ remains the same for this range of U's.

3. The behavior of γ(r,U): General case

We are now in the position to sketch the behavior of $\gamma(r,U)$. Although we have considered specifically the case $0 < \gamma < 1$, i.e., $0 < U < r/(1-r)$, the previous considerations can be straightforwardly generalized to arbitrary n. For example, if $(n-1)r/(1-r) < U < nr/(1-r)$, the functional iteration of the model [Eqs. (4) and (7)] can be generalized to

$$e_{i+1} = (e_i + 1) r^{l_i} + (n-1) \frac{r}{1-r} (1 - r^{l_i}), \tag{23}$$

$$l_i = \mathrm{int}\left(\frac{\ln[\tilde{U}/(\tilde{e_i} + 1)]}{\ln r} \right), \tag{24}$$

where

$$\tilde{U} = U - (n-1) \frac{r}{1-r}, \tag{25}$$

$$\widetilde{e_i} = e_i - (n-1)\frac{r}{1-r}. \tag{26}$$

The trivial solution of Eqs. (12) and (13) can be generalized to

$$\gamma = (n-1) + \frac{1}{l(n)} \quad \text{if} \quad r\frac{r^{l(n)}}{1-r^{l(n)}} \leqslant \tilde{U} \leqslant \frac{r^{l(n)}}{1-r^{l(n)}}, \tag{27}$$

where

$$l(n) = \mathrm{int}\left(\frac{\ln[\tilde{U}/(\tilde{U}+1)]}{\ln r}\right). \tag{28}$$

Additionally, Eq. (19) applies for arbitrary (γ, n).

Also this general case is easy to solve numerically in a manner similar to the case $0 < \gamma < 1$ explained in the preceding subsection. For illustration, the solid lines in Fig. 2(a) show the results for γ using the numerical iteration of Eqs. (23) and (24). We find that the iterates of γ agree excellently with the results from the straightforward simulations also for arbitrary γ.

In summary, we find both numerically, as well as analytically, that for $(n-1)r/(1-r) < U < nr/(1-r)$, $n-1 < \gamma < n$ gets all the rational values in a hierarchical manner: specifically, $n-1+1/(l+1) < \gamma \leqslant n-1+1/l$, in a segment of U space, $r^{l(n)+1}/(1-r^{l(n)+1}) < U \leqslant r^{l(n)}/(1-r^{l(n)})$. The behavior of the system is determined by a dimensionless parameter $l(n)$, which varies nonmultiplicatively as a function of n.

IV. CONNECTION TO A 1D ISING MODEL WITH LONG-RANGE INTERACTIONS

We find that there is a close connection between the present model and the one-dimensional (1D) Ising system of Ref. [16]. This section describes the similarities, and the differences, between these models.

Reference [16] deals with the Hamiltonian $\mathcal{H}$,

$$\mathcal{H} = \sum_i HS_i + \frac{1}{2}\sum_{i,j} J(|i-j|)(S_i+1)(S_j+1), \tag{29}$$

where the first summation is over K spins, $S_i = \pm 1$, in a chain with periodical boundaries, H is the magnetic field, and the second sum counts all the pairs of the ''up'' spins interacting via a long-range interaction J, which only depends on the mutual distance between the spins. Assuming that each site may occupy only a single spin, the problem of minimizing the classical Hamiltonian $\mathcal{H}$ is equivalent to arranging a number of charged particles on K sites such that the interaction energy is minimized. In this case an occupied (vacant) site corresponds to $S=1$ $(S=-1)$. The latter problem is solved by Hubbard [21] and by Pokrovski and Uimin [22], yielding that the arrangement of the up spins is periodic at the ground state of $\mathcal{H}$, such that there exists a unit cell of length L, with N up spins, which repeats itself *ad infinitum*. These periodic structures arise from the competition between different spatial periodicities, and the fraction of the up spins, $q = N/L$, may have all possible rational values. As shown in Ref. [16], a commensurate phase characterized by a given q is stable as long as it costs energy to flip any spin, and rearrange the new configuration to minimize the energy. Specifically, Ref. [16] calculates these energy costs for a spin flipping, and finds them positive for a range of fields H, whose width is given by $(K \to \infty)$

$$\Delta H(q = N/L) = 2\sum_{p=1}^{\infty} pL[J(pL+1) + J(pL-1) - 2J(pL)]. \tag{30}$$

Equation (30) should be compared with Eq. (20), $\Delta U = (1-r)\sum_{p=1}^{\infty} r^{pL}$. This comparison suggests that there is a class of interactions J for which the Ising model behaves similarly to the present model.

For example, assuming that the interaction has a (somewhat artificial) form $J(x) = (1-r^L)r^x$, we find that Eq. (30) reads

$$\Delta H = 2\frac{1-r^L}{(1-r)^2}\sum_{p=1}^{\infty} pLr^{pL-1} = 2L\,\frac{1-r}{r}\,\frac{r^L(1-r)}{(1-r^L)}. \tag{31}$$

Therefore, for this specific choice of interaction potential J, the stability region for the Ising model is similar to our stability condition Eq. (20), apart from the prefactor $2L(1-r)/r$. Additionally, using Eq. (14), we find that the average energy in the sequence $\{e_i\}$ can be written in a form

$$\langle e_i \rangle \approx \sum_{1 \leqslant i < j \leqslant N} J(|i-j|) + \frac{r^L}{1-r^L}. \tag{32}$$

This suggests that there exist a set of analogous quantities: γ, U, and e_i are analogous to magnetization M $(M = 2q-1)$, magnetic field H, and interaction energy of a spin, respectively.

However, the most important difference between these models is that the specific mechanism which determines the location of the commensurate phase boundaries are definitely different. For the Ising model the stability region is determined by the energy cost of the spin flipping, whereas the stability criterion for the present model is the requirement that we need to find a self-consistent solution for $\{N, l_i, e_i\}$, which is periodic in the energy space. In fact, we find that the smooth surface which has only steps of two different sizes minimizes the fluctuations of the energy, i.e., the proper solution for the grain energies $\{e_i\}$ needs to be bounded between $[U, U/r[$.

V. CONCLUSION

We have studied a simple model for the surface of a granular heap. The model includes the considerations of the dissipation of the energy in the particle-particle collisions, and the sticking of the particles to the pile. For given (r, U), this deterministic model evolves into a steady state, from which physical observables, such as the angle of repose, can be determined. Within this simple model, the dependence of $\gamma(r, U)$ may therefore enlighten how the angle of repose depends on the properties of the granular system, including the shape (U) and dissipation (r) between the granulates.

We find that the angle of repose of the pile behaves as a complete devil's staircase, and present numerical and analytical considerations which characterize the properties of this staircase. We find that the sizes of the steps on the surface depend on (r,U) in a complicated manner, and this results to a fascinating hierarchical structure in the $\gamma(r,U)$.

ACKNOWLEDGMENTS

We acknowledge useful discussions with C. Criado, S. Luding, and M. Rimmele. J.J.A. is grateful for an *Ayuda parcial* (PB91-0709) and a grant from DGICYT. J.-P.-H. gratefully acknowledges financial support from the European Union (Training and Mobility for Researchers) under Contract No. ERBFMBICT971935.

APPENDIX: OUTLINE OF THE EXPLICIT SOLUTION FOR $U_{\mathrm{min,max}}$

This appendix gives the details of the solution of $U_{\mathrm{min,max}}$ for several values of γ. In particular, we cover the cases for which $\gamma=(1+p)/[(1+p)l+1]$, where either p or p^{-1} is an integer. We do not consider the case $p=0$, since that corresponds to the trivial solution of Eq. (12). Additionally, the most general solution would correspond to the considerations where p is an arbitrary rational number, but we do not discuss that solution here.

For nonzero p, we have $r^{l+1}/(1-r^{l+1})<U<r[r^l/(1-r^l)]$. Since there are no integers which satisfy Eq. (10), the steps of the surface appear with two different intervals l and $l+1$, where $l=\mathrm{int}\{\ln[U/(U+1)]/\ln r\}$. For any e_i, l_i may have either one of these values, depending on which choice fulfills the condition $U\leqslant e_{i+1}=(e_i+1)r^{l_i}\leqslant U/r$. Let m (n) be the number of intervals of length l $(l+1)$, for which choice $L=(m+n)l+n$, $\gamma=(m+n)/[(m+n)l+n]$, and the periodic boundaries read $e_{m+n+1}=e_1$. Using Eq. (4) we find

$$e_{m+n+1}=(e_1+1)r^L+\sum_{p=1}^{m+n} r^{\sum_{q=p}^{m+n} l_q}=e_1. \tag{A1}$$

Additionally, due to the periodic boundaries, we may choose that e_1 is the smallest energy in the sequence $\{e_i\}$.

Since Eq. (A1) is relatively complicated, we shall limit ourselves to a very special case of the energy landscape. In what follows we consider only the case where $m=1$ or $n=1$ (this corresponds to $\gamma=(1+p)/[(1+p)l+1]$, with $p=m/n$). After this simplification in the algebra one has the freedom to set $l_i=l$ $(l_i=l+1)$ for $i\leqslant m$ $(i>m)$. However, this assumption is valid *only* if the energy landscape has this kind of very simple structure where there is only one hill in the sequence $\{e_i\}$.

In other words, starting from e_1 close to U, there are first m steps with intervals l, where m is the smallest integer which obeys

$$U/r<(e_{m+1}+1)r^l\leqslant U/r^2, \tag{A2}$$

with

$$\max\{e_i\}=e_{m+1}=e_1r^{ml}+\sum_{p=1}^{m} r^{pl}=e_1r^{ml}+r^l\frac{1-r^{ml}}{1-r^l}. \tag{A3}$$

Subsequently, there are n steps with intervals $l+1$, and the energy decreases back to the original value

$$\begin{aligned} e_{n+m+1}&=e_{m+1}r^{n(l+1)}+\sum_{p=1}^{n} r^{p(l+1)}\\ &=e_{m+1}r^{n(l+1)}+r^{l+1}\frac{1-r^{n(l+1)}}{1-r^{l+1}}\\ &=e_1r^{(m+n)l+n}+r^{nl+n+l}\frac{1-r^{ml}}{1-r^l}\\ &\quad+r^{l+1}\frac{1-r^{n(l+1)}}{1-r^{l+1}}=e_1. \end{aligned} \tag{A4}$$

After a straightforward calculation one finds that

$$\min\{e_i\}=e_1=\frac{r^l}{1-r^{(m+n)l+n}}\left(r^{nl+n}\frac{1-r^{ml}}{1-r^l}+r\frac{1-r^{nl+n}}{1-r^{l+1}}\right). \tag{A5}$$

Equations (A3) and (A5) determine the range of the parameters, $U_{\mathrm{min}}=r\max\{e_i\}\leqslant U\leqslant\min\{e_i\}=U_{\mathrm{max}}$, which correspond to the same $\gamma=(1+p)/[(1+p)l+1]$ (with $p=m/n$). However, since we have assumed a special form of the energy landscape, Eqs. (A3) and (A5) are valid only if at least either m or n is unity. This implies that either p or p^{-1} is an integer. For example, if $p=1$, we find that $\gamma=2/(2l+1)$ for

$$\frac{r^{l+1}}{1-r^{2l+1}}(1+r^{l+1})\leqslant U\leqslant\frac{r^{l+1}}{1-r^{2l+1}}(1+r^l). \tag{A6}$$

[1] T. Boutreaux and P. G. de Gennes, J. Phys. I **6**, 1295 (1996).
[2] H. A. Makse, S. Havlin, P. R. King, and H. E. Stanley, Nature (London) **386**, 379 (1997).
[3] D. A. Head and G. J. Rodgers, Phys. Rev. E **56**, 1976 (1997).
[4] M. Bretz, Phys. Rev. Lett. **69**, 2431 (1992).
[5] V. G. Benza, Phys. Rev. E **48**, 4095 (1993).
[6] J. J. Alonso and H. J. Herrmann, Phys. Rev. Lett. **76**, 4911 (1996).
[7] Y. Grasselli and H. J. Herrmann, Physica A **246**, 301 (1997).
[8] J. Wittmer, P. Claudin, M. Cates, and J.-P. Bouchard, Nature (London) **382**, 336 (1996); J. Wittmer, M. Cates, and P. Claudin, J. Phys. I **7**, 39 (1997).
[9] J. R. L. Allen, Geol. Mijnbouw **49**, 13 (1970).
[10] D. J. Hornbaker, R. Albert, I. Albert, A.-L. Barabasi, and P. Schiffer, Nature (London) **387**, 765 (1997).
[11] C. Giovannella, F. Ritort, and A. Giannelli, Europhys. Lett. **29**, 419 (1995), and references therein.
[12] S. Shapiro, Phys. Rev. Lett. **11**, 80 (1963).
[13] P. A. Crowell and J. D. Reppy, Phys. Rev. Lett. **70**, 3291 (1993); G. T. Zimanyi, P. A. Crowell, R. T. Scalettar, and G.

G. Batrouni, Phys. Rev. B **50**, 6515 (1994).
[14] *Progress in Crystal Growth and Characterization*, edited by P. Krishna (Pergamon, Oxford, 1983), Vol. 7; A. Loiseau, G. Van Tendeloo, R. Portier, and F. Ducastelle, J. Phys. (Paris) **46**, 595 (1985).
[15] P. Bak, Phys. Today **9(12)**, 38 (1986).
[16] P. Bak and R. Bruinsma, Phys. Rev. Lett. **49**, 249 (1982); R. Bruinsma and P. Bak, Phys. Rev. B **27**, 5824 (1983).
[17] J. von Boehm and P. Bak, Phys. Rev. Lett. **42**, 122 (1979); P. Bak and J. von Boehm, Phys. Rev. B **21**, 122 (1980).
[18] J. Yeomans, in *Solid State Physics: Advances in Research and Applications* (Academic Press, New York, 1988), Vol. 41.
[19] M. Rimmele, M.Sc. thesis, University of Stuttgart, 1997 (in German); M. Rimmele *et al.* (unpublished).
[20] K. Goldberg, M. Newman, and E. Haynsworth, in *Handbook of Mathematical Functions*, edited by M. Abramowitz and I. A. Stegun (Dover, New York, 1972).
[21] J. Hubbard, Phys. Rev. B **17**, 494 (1978).
[22] V. L. Pokrovski and G. V. Uimin, J. Phys. C **11**, 3535 (1978).